



OPEN

Mycobacterium abscessus biofilms have viscoelastic properties which may contribute to their recalcitrance in chronic pulmonary infections

Erin S. Gloag¹, Daniel J. Wozniak^{1,2}, Paul Stoodley^{1,3,4} & Luanne Hall-Stoodley¹✉

Mycobacterium abscessus is emerging as a cause of recalcitrant chronic pulmonary infections, particularly in people with cystic fibrosis (CF). Biofilm formation has been implicated in the pathology of this organism, however the role of biofilm formation in infection is unclear. Two colony-variants of *M. abscessus* are routinely isolated from CF samples, smooth (Ma^{Sm}) and rough (Ma^{Rg}). These two variants display distinct colony morphologies due to the presence (Ma^{Sm}) or absence (Ma^{Rg}) of cell wall glycopeptidolipids (GPLs). We hypothesized that Ma^{Sm} and Ma^{Rg} variant biofilms might have different mechanical properties. To test this hypothesis, we performed uniaxial mechanical indentation, and shear rheometry on Ma^{Sm} and Ma^{Rg} colony-biofilms. We identified that Ma^{Rg} biofilms were significantly stiffer than Ma^{Sm} under a normal force, while Ma^{Sm} biofilms were more pliant compared to Ma^{Rg} , under both normal and shear forces. Furthermore, using theoretical indices of mucociliary and cough clearance, we identified that *M. abscessus* biofilms may be more resistant to mechanical forms of clearance from the lung, compared to another common pulmonary pathogen, *Pseudomonas aeruginosa*. Thus, the mechanical properties of *M. abscessus* biofilms may contribute to the persistent nature of pulmonary infections caused by this organism.

In the cystic fibrosis (CF) lung, due to genetic mutations in the cystic fibrosis transmembrane regulator (CFTR) ion channel responsible for this disease, the mucus lining of the airways becomes dehydrated and highly viscous, leading to impaired clearance and accumulation. This provides a niche that can be readily colonized by inhaled microorganisms, which form biofilm aggregates within the accumulated mucus layer^{1,2}. These biofilms lead to recurrent progressive infections, inflammation, bronchiectasis and, eventually, respiratory failure. Nontuberculous mycobacteria (NTM) are an increasingly common complication in CF, now ranking as the third most frequent cause of lung infection in people with CF³⁻⁵. *Mycobacterium abscessus* infection is particularly challenging, infecting younger people with CF and resulting in a poorer prognosis than those infected with other NTM^{3,4,6-8}. However, the mechanisms underlying the rising incidence of *M. abscessus* infection in people with CF remain ill-defined^{9,10}.

Mycobacterium abscessus has two distinct colony variants, based on the presence (smooth morphotype; Ma^{Sm}) or absence (rough morphotype; Ma^{Rg}) of cell wall glycopeptidolipids (GPLs)^{11,12}. The prevailing view of chronic *M. abscessus* infection is that Ma^{Sm} is a noninvasive, biofilm-forming, persistent phenotype, and Ma^{Rg} is an invasive phenotype that is unable to form biofilms. We have previously shown, however, that Ma^{Rg} is hyper-aggregative and is capable of forming biofilm aggregates, which are significantly more tolerant than planktonic *M. abscessus* to acidic pH, hydrogen peroxide, or antibiotic treatment¹¹. These studies indicate that development of biofilm aggregates contribute to the persistence of *M. abscessus* in the face of antimicrobial agents, regardless of morphotype. Antibiotic regimens that reliably cure *M. abscessus* infections are lacking. A better understanding

¹Department of Microbial Infection and Immunity, The Ohio State University, 711 Biomedical Research Tower, 460 W 12th Avenue, Columbus, OH, USA. ²Department of Microbiology, The Ohio State University, Columbus, OH 43210, USA. ³Department of Orthopedics, The Ohio State University, Columbus, OH 43210, USA. ⁴National Biofilm Innovation Centre (NBIC) and National Centre for Advanced Tribology at Southampton (nCATS), University of Southampton, Southampton SO17 1BJ, UK. ✉email: Luanne.Hall-Stoodley@osumc.edu

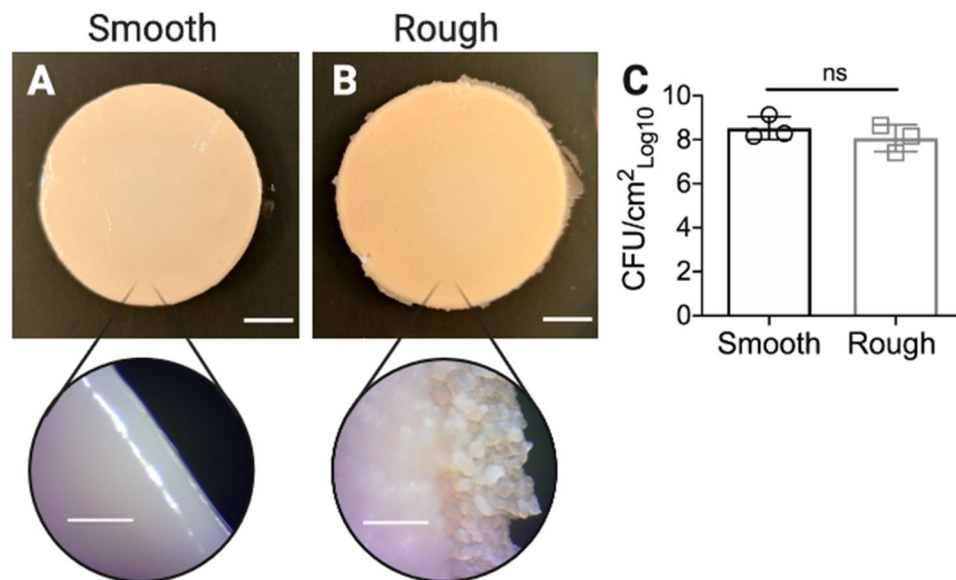


Figure 1. Morphology of *Ma*Sm and *Ma*^{Rg} colony-biofilms. (A) *Ma*Sm and (B) *Ma*^{Rg} were grown on nitrocellulose membranes for 4 days, transferring the membranes onto fresh media after 48 h. Colony-biofilms were then imaged to visualize the macroscopic morphology. Scale bar indicates 5 mm, and 0.5 mm for the zoomed insets. (C) To assess the biomass and if each variant was stable during biofilm formation, 4 day *M. abscessus* biofilms were enumerated for CFUs. Evidence of phenotypic changes of the colony morphologies for either was not observed at 37°C over 4 days. Statistical analysis was performed using a Student's t-test; ns indicated not significant. N = 3.

of the the biofilm biology of this organism and its ability to cause persistent pulmonary infections is needed to explore new treatment strategies^{13,14}.

The study of biofilm mechanics has gained interest, as it is being realized that these properties are important for understanding biofilm biology and how biofilms respond to chemical and mechanical forms of eradication¹⁵. Interestingly, changes in colony morphology have been correlated to differences in biofilm formation¹⁶, and differences in biofilm mechanics^{17,18}. We therefore hypothesized that the biofilms of *Ma*Sm and *Ma*^{Rg} may have different mechanical properties, due to their distinct colony morphologies, and that these properties may help to account for the persistence of infection caused by this organism. In the present study, we used mechanical indentation and shear rheometry to evaluate the viscoelastic properties of *Ma*Sm and *Ma*^{Rg} biofilms. We also used known concepts of mucus viscoelasticity to predict how effectively *M. abscessus* biofilms may be cleared from the lung by mucociliary and cough clearance. Our findings support the hypothesis that biofilm viscoelasticity could contribute to the persistence of biofilm-associated infections^{15,19}, and provides novel insight into why *M. abscessus* may be such a persistent pathogen in airway infection in people with CF.

Results

***Ma* colony-biofilms maintain the distinct morphologies of *Ma*Sm and *Ma*^{Rg} variants.** *Mycobacterium abscessus* is a rapidly growing NTM, typically showing colony morphology by 4 days on agar media. To test the hypothesis that biofilms of *Ma*Sm and *Ma*^{Rg} variants might differ in their mechanical properties, uniaxial indentation and shear rheology was performed on 4 day *M. abscessus* colony-biofilms (See Supplementary Methods). As this is the first time that we have used this biofilm model for *M. abscessus*, we examined the colony-biofilms after 4 days of growth (Fig. 1). Macroscopically, biofilm formation was evident, covering the filter. Biofilm morphology maintained the characteristic phenotypes of each variant¹¹. That is, biofilms of *Ma*Sm, had a smooth, almost mucoid appearance (Fig. 1A), while *Ma*^{Rg} biofilms showed a cauliflower-like morphology (Fig. 1B) in agreement with our previous study showing cording at the periphery of *Ma*^{Rg} colonies¹¹. Importantly, when these colony-biofilms were disrupted, and plated to observe single cells, the number of cells within the biofilm was similar across the two variants, and no reversion across phenotypes was observed during this time (Fig. 1C), demonstrating that during the 4 day biofilm growth period, each variant was stable.

***Ma*^{Rg} biofilms are stiffer than *Ma*Sm biofilms in uniaxial compression.** To determine the stiffness of *M. abscessus* biofilms under a normal force (force that is applied perpendicular to the surface), uniaxial indentation was performed on 4 day *M. abscessus* colony-biofilms. During this analysis, biofilms are compressed and the required force is measured. This analysis is also used to determine the biofilm thickness, which revealed that biofilms of each variant were of similar thickness (Fig. 2A), consistent with the observation that biofilms had a similar number of CFUs (Fig. 1C). Stress–strain curves revealed that *Ma*Sm and *Ma*^{Rg} biofilms displayed a 'J-shaped' curve, where the biofilms became progressively stiffer as they were compressed (Fig. S1). Stress–strain curves also revealed that there were significant mechanical differences between *Ma*Sm and *Ma*^{Rg} biofilms (Fig. 2B;

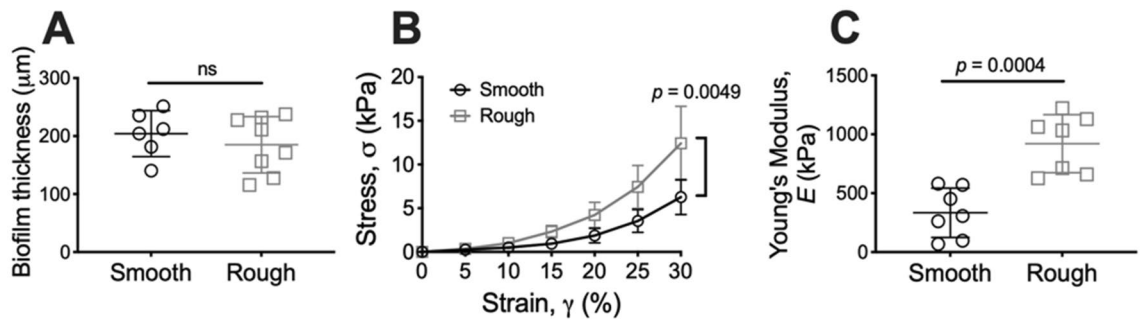


Figure 2. Ma^{Rg} colony-biofilms are stiffer compared to Ma^{Sm} biofilms in compression. (A) Thickness and (B) stress–strain curves of 4 day *M. abscessus* colony-biofilms determined from uniaxial indentation analysis. (C) Young's modulus of *M. abscessus* biofilms, determined from the lower linear portion of the force–displacement curve, corresponding to 0–30% strain. The full stress–strain curve, up to 100% strain is represented in Fig. S1. $N = 4$; data presented as individual data points with mean \pm SD. Statistical analysis was performed using a Student's t-test; ns indicates not significant.

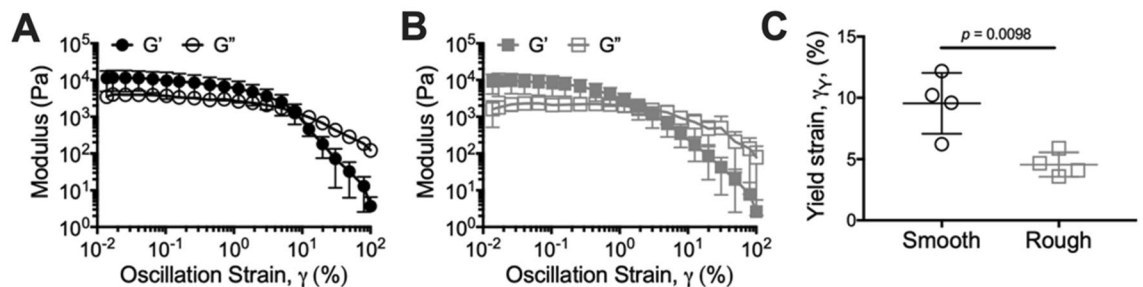


Figure 3. Ma^{Sm} colony-biofilms are more pliant than Ma^{Rg} biofilms in shear. Strain sweep profiles of 4 day (A) Ma^{Sm} and (B) Ma^{Rg} colony-biofilms. $N = 4$; data presented as mean \pm SD; G' = storage modulus and G'' = loss modulus. (C) Yield strain of *M. abscessus* colony-biofilms determined from (A) and (B). $N = 4$; data presented as individual data points with mean \pm SD. Statistical analysis was performed using a Student's t-test.

$p = 0.0049$). To quantify these differences, the Young's modulus was determined from the lower linear portions of the curve, which revealed that the Young's modulus of Ma^{Rg} biofilms was approximately two-fold greater than Ma^{Sm} biofilms. This indicates that Ma^{Rg} biofilms were significantly stiffer under uniaxial compression, compared to Ma^{Sm} biofilms (Fig. 2C; $p = 0.0004$).

***M. abscessus* biofilms are highly viscoelastic and Ma^{Sm} biofilms are more pliant than Ma^{Rg} under shear.**

To examine the mechanical properties of *M. abscessus* colony-biofilms in further detail, Ma^{Sm} and Ma^{Rg} biofilms were analyzed using spinning-disc rheology. For these analyses a shear force (a force that is applied parallel to a surface) is applied and the resulting stress or strain is measured (See Supplementary Methods). Oscillatory strain sweeps were performed, where the oscillatory strain was incrementally increased and the storage (G') and loss (G'') moduli measured, which reflect the elastic and viscous response, respectively¹⁵. The measured storage and loss moduli plateaus were similar for Ma^{Sm} and Ma^{Rg} biofilms (Fig. 3A,B), suggesting that biofilms of each variant behaved similarly within the linear viscoelastic region. From this analysis we determined the yield strain, which represents the strain where the biofilm integrity begins to break down, due to the increasing applied strain, and transitions to fluid-like behavior²⁰. Interestingly, the yield strain of Ma^{Sm} biofilms was significantly greater than Ma^{Rg} biofilms (Fig. 3C; $p = 0.0098$). This suggests that Ma^{Sm} biofilms are more pliant than Ma^{Rg} biofilms, and that Ma^{Sm} biofilms can be deformed to a greater extent before cohesive failure occurs. This is also consistent with the Young's modulus of these biofilms, which indicated that Ma^{Sm} biofilms can be compressed more readily compared to Ma^{Rg} biofilms (Fig. 2C).

Oscillatory frequency sweeps were also performed, where the oscillatory frequency was incremented under a consistent applied strain, and the storage and loss moduli measured. Across the range of frequencies analyzed, the storage and loss moduli were relatively independent of frequency, with the storage modulus greater than the loss modulus for both *M. abscessus* variant biofilms (Fig. 4A,B). This indicates that both Ma^{Sm} and Ma^{Rg} biofilms displayed elastic behavior that was dominant across the analyzed conditions. There were no significant differences between the mechanical behavior of Ma^{Sm} and Ma^{Rg} biofilms using this analysis (Fig. 4C,D). However, compared to Ma^{Sm} biofilms, Ma^{Rg} biofilms trended toward a reduced loss modulus across the analyzed frequencies (Fig. 4D).

Theoretical indices suggest that *M. abscessus* biofilms, independent of morphotype, may resist clearance from the lung. To determine if the mechanical properties of *M. abscessus* biofilms may

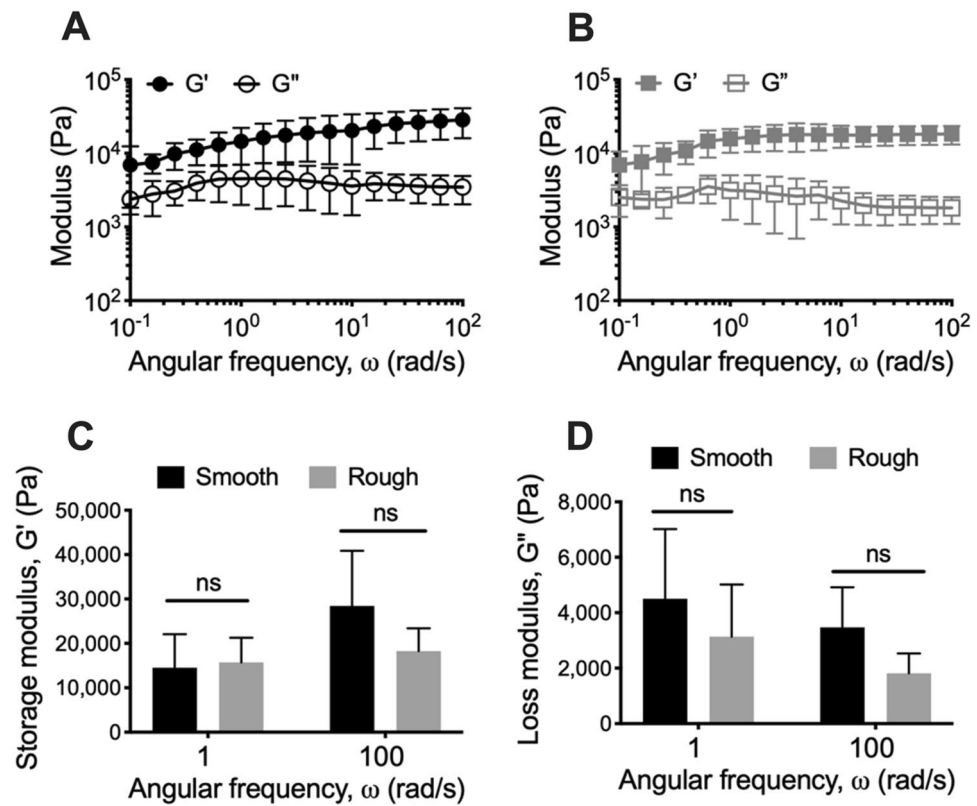


Figure 4. *M. abscessus* colony-biofilms are highly viscoelastic. Frequency sweep profiles of 4 day (A) Ma^{Sm} and (B) Ma^{Rg} colony-biofilms. G' = storage modulus and G'' = loss modulus (C) Storage and (D) and loss moduli values at 1 and 100 rad/s. N = 4; data presented as mean \pm SD. Statistical analysis was performed using a Student's t-test; ns indicates not significant.

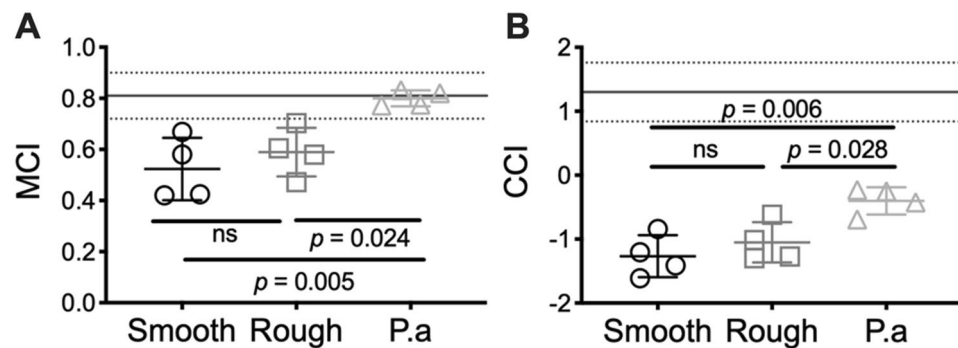


Figure 5. *M. abscessus* colony-biofilms have reduced theoretical mucociliary and cough clearance index. (A) Mucociliary and (B) cough clearance index of 4-day *M. abscessus* and *P. aeruginosa* (P.a) colony-biofilms. Lines at (A) and (B) are the MCI (0.81 ± 0.09) and CCI (1.3 ± 0.46), respectively, of sputum collected from patients with CF, previously determined by⁵⁴. N = 4; data presented as individual data points with mean \pm SD. Statistical analysis was performed using a one-way ANOVA with a Tukey's post-hoc test; ns indicates not significant.

correlate with recalcitrance of *M. abscessus* in pulmonary infections, we calculated the mucociliary (MCI) and cough (CCI) clearance index, according to Eqs. (2) and (3), using values from the frequency sweep analysis of these biofilms (Fig. 4). The MCI and CCI were developed to correlate sputum viscoelasticity to predicted levels of clearance from the lung via either mechanism^{21,22}. The MCI and CCI of Ma^{Sm} and Ma^{Rg} biofilms were similar. However, due to the highly viscoelastic behavior of both colony variant biofilms (Fig. 4A,B), the indices were less than the MCI and CCI reported for sputum collected from people with CF (Fig. 5; line).

To compare *M. abscessus* biofilms to the biofilms of another common pathogen causing chronic pulmonary infections in people with CF, we analyzed 4 day wild type *Pseudomonas aeruginosa* colony-biofilms²³. *P. aeruginosa* is considered a model organism for biofilm formation, and we have previously determined the MCI and CCI for this organism¹⁷. Using the same testing conditions for *M. abscessus* biofilms described here, we performed oscillatory frequency sweeps on 4 day wild type *P. aeruginosa* colony-biofilms (See Supplementary Results; Fig. S2), and similarly determined the MCI and CCI for comparison (Fig. 5). The indices of Ma^{Sm} and Ma^{Rg} biofilms were significantly less than that determined for wild type *P. aeruginosa* biofilms (Fig. 5). This suggests that *M. abscessus* biofilms may be more resistant to mechanical clearance from the lung, compared to other common pulmonary pathogens, such as *P. aeruginosa*.

Discussion

Compared to other biofilm forming organisms, such as *P. aeruginosa*, the understanding of biofilm formation and the role of biofilms in infection of NTMs is limited. It is important to understand biofilm mechanics from a biofilm biology stand-point, as these properties dictate the stability of the three-dimensional community structure¹⁵. We therefore set out to analyze the mechanical properties of *M. abscessus* in vitro biofilms to gain a better understanding of the biofilm biology of this organism. We found that Ma^{Rg} colony-biofilms were stiffer under normal forces (Fig. 2C), while Ma^{Sm} colony-biofilms were more pliable under both normal and shear forces (Figs. 2C, 3C). In contrast to the uniaxial indentation analysis (Fig. 2), oscillatory frequency sweeps indicated that there were no significant difference in the viscoelasticity of Ma^{Sm} and Ma^{Rg} biofilms under shear forces (Fig. 4). This indicates that *M. abscessus* biofilms were anisotropic, in that they have different mechanical properties when exposed to either a normal or shear force.

Earlier research by others suggested that only Ma^{Sm} variants formed biofilms and speculated that GPL expression enhanced sliding motility in CF mucus, making it better adapted to behave as a colonizing, biofilm-forming phenotype^{24,25}. However, we have previously shown that the rough morphotype is hyper-aggregative¹¹, indicating that each colony morphology variant is capable of forming biofilm aggregates. The finding here that Ma^{Sm} colony-biofilms were more pliable under both normal and shear forces (Figs. 2C, 3C) suggests that GPL likely affects the mechanical properties of *M. abscessus* biofilms. Further studies are needed to better understand the relationship of *M. abscessus* cell wall determinants, such as lipids, GPLs, and extracellular polymeric substance (EPS) with biofilm function and is the focus of future studies.

Uniaxial indentation, revealed that Ma^{Sm} and Ma^{Rg} biofilms each displayed a 'J-shaped' curve in response to increasing compression (Fig. 2B). This response is typical of biological materials, and has previously been observed for a number of different types of bacterial biofilms^{17,26–28}. The Young's modulus of Ma^{Sm} and Ma^{Rg} colony-biofilms, determined here, is similar to that reported for *Streptococcus mutans* hydrated biofilms²⁹, *P. aeruginosa* colony-biofilms¹⁷, and surface adhered *Staphylococcus aureus*, *Staphylococcus epidermidis* and *Streptococcus salivarius* cells³⁰.

Interestingly, Ma^{Sm} and Ma^{Rg} colony-biofilms have a storage modulus, which describes the elastic solid-like behavior³¹, approximately tenfold greater than that previously observed for other bacterial biofilms (Fig. S2A)^{17,18,20,32–40}. This suggests that *M. abscessus* biofilms, regardless of the morphotype, are highly viscoelastic, and much stiffer than biofilms formed by other bacterial pathogens. It would, therefore, be of interest to compare the mechanical properties of other NTM biofilms, as well as other biofilms that have a lipid dominant EPS, to determine the contributions of lipid content to the EPS and to the biofilm mechanical properties. It is interesting to speculate that different host niches in the lung (or other infection sites) may favor stiffer or softer biofilms depending on different shear and chemical micro environments. However, this requires further clinical work.

Viscoelasticity is a property common to biofilms, suggesting that it is an adaptive trait of these microbial communities¹⁵. It has therefore been predicted that biofilm viscoelasticity, not only is important from a biofilm biology stand-point, but also when considering microbial survival⁴¹. Understanding how biofilm mechanics impacts microbial survival in an infection is still unclear. However, there is a growing consensus that these properties are important for resisting both mechanical and chemical methods of eradication^{15,19}. To gain further insight into how the mechanics of *M. abscessus* biofilms may influence the recalcitrance of these infections, we used known, well-established concepts of mucus viscoelasticity to draw new hypotheses that may be relevant to *M. abscessus* biofilms in vivo, in the context of mechanical clearance from the lung. Changes in mucus viscoelasticity in CF are attributed to mucus hyper-secretion and changes to mucus composition, impeding mucus clearance by both mucociliary and cough clearance⁴². MCI and CCI are theoretical indices that were developed from in vitro lung clearance models to correlate viscoelastic properties of expectorated mucus with predicted levels of clearance from the lung^{21,22}. These indices have been used to assess the efficiency of mucolytics for therapy regimes for people with CF⁴³. MCI predicts that mucus elasticity correlates to improved mucociliary clearance by promoting efficient cilia beating^{21,44}, while CCI predicts that mucus viscosity correlates to improved cough clearance by promoting mucus-airflow interactions^{44,45}. We previously used these known relationships between mucus viscoelasticity and clearance, and applied these concepts to *P. aeruginosa* colony-biofilms, to determine if the viscoelastic properties of bacterial biofilms could likewise theoretically impact mechanical clearance from the lung¹⁷. We identified that elastic non-mucoid *P. aeruginosa* biofilms had a reduced CCI, while mucoid *P. aeruginosa* biofilms that had a low viscosity, had both a reduced MCI and CCI¹⁷. Here we determined the MCI and CCI of *M. abscessus* biofilms, and observed that they had an even lower or negative CCI compared to *P. aeruginosa*, attributed to the high viscoelasticity of these biofilms (Fig. 5B). This indicates that *M. abscessus* biofilms of each morphotype may resist clearance from the lung by cough. These findings provide novel insight into possible reasons why *M. abscessus* is a persistent and difficult to treat pulmonary pathogen.

A longitudinal rheological study of sputum from CF patients indicated that both viscosity and elasticity increase during pulmonary exacerbations, suggesting that CF sputum viscoelasticity is linked to disease state and airflow obstruction⁴⁶. By applying known concepts of mucus rheology to biofilm mechanics and infection, our findings provide a novel way to understand *M. abscessus* biofilms and their recalcitrance. Moving forward, it will be important to develop in vitro and in vivo models of biofilm-mucus interactions to explore the hypotheses drawn from this work. More broadly, the impact of evaluating bacterial biofilm mechanical properties offers new avenues for the treatment of intractable pulmonary infections. Disruption of *M. abscessus* aggregates increased susceptibility to several antibiotics¹³. Moreover, liposomes, lipid nanoparticles and nanoparticle lipid carriers are being evaluated for pulmonary use⁴⁷. This approach has been used on biofilms of *Burkholderia cepacia* complex, as well as *S. aureus* and *P. aeruginosa* biofilms in vitro^{48,49}. These products not only have the potential to reduce exposure to high concentrations of antimicrobial agents following aerosol administration by reducing toxicity, but particularly relevant to NTM antibiotic therapy, might ameliorate the severe side effects often associated with antimycobacterial treatment. This strategy could further be used to target NTM, which have a high lipid content, to facilitate cohesive failure of biofilm aggregates in the lung in addition to delivering targeted antibiotics.

Materials and methods

***M. abscessus* culture and biofilm model.** The colony-biofilm model was used here due to the established utility of this model for rheological analysis of biofilms^{17,50} (See Supplementary Methods). Colony-biofilms were grown as previously described with modifications¹⁷. Briefly, *M. abscessus* cultures were prepared by inoculating a 10 μ L loop of isolated *Ma*Sm or *Ma*^{Rg} from 7H10 agar plates into 7H9 without tween media and a single cell suspension prepared as described¹¹. Cultures were normalized to an OD₆₀₀ of 0.15–0.2 and 100 μ L was pipetted onto sterile nitrocellulose filter membranes (25 mm, 0.45 μ m pore size; Millipore) and incubated at 37 °C, 5% CO₂ under humidified conditions for 4 days. This time point was selected as it provided sufficient biomass necessary for rheological analysis, while maintaining the characteristic morphology of *Ma*Sm or *Ma*^{Rg} variants. Colony-biofilms of PAO1 *P. aeruginosa* were grown as previously described¹⁷.

Colony-biofilms were imaged using a Stereo Microscope (AmScope) fitted with a Microscope Digital Color CMOS camera (AmScope). Images were processed in FIJI⁵¹. Figure was compiled in Biorender.com.

To assess the number of CFU/cm² on sterile membranes after 4 days, colony-biofilms were scraped and transferred to 5 mL of 7H9 + tween 80 and vortexed with glass beads to disperse cells from the biofilm¹¹. Cell suspensions were serially diluted and enumerated for CFUs in triplicate on 7H10 agar plates. To determine if either variant converted/reverted to another colony variant during biofilm growth, colony morphology was also assessed and verified by sub-culturing three colonies per replicate to ensure that the colony morphology was stable. CFUs were plated to 10⁸ dilution and colonies were streaked to isolation to validate colony variants.

Rheometry apparatus. A Discovery Hybrid Rheometer-2 with a heat exchanger attached to the Peltier plate (TA Instruments) was used for all rheological measurements. For uniaxial indentation and spinning disc measurements (See Supplementary Methods), the rheometer was fitted with an 8 mm and 25 mm sand-blasted Smart Swap geometry, respectively. All measurements were performed at 37 °C, with the Peltier plate covered with a moist Kimwipe to prevent dehydration of the colony-biofilm. TRIOS v4 (TA instruments) software was used.

Uniaxial indentation measurements. Uniaxial indentation measurements were performed under compression using an approach rate of 1 μ m/s. Two colony-biofilms were analyzed per biological replicate (total of 4 biofilms analyzed), with two measurements per biofilm. The point of contact with the biofilm was determined to be where the force began to increase after the initial point of pull-on adhesion. Force–displacement curves were converted to stress–strain curves, for ease of comparison, as previously described¹⁷. The Young's modulus was calculated according to Eq. (1)⁵²:

$$E = \frac{\text{slope} \cdot (1 - \nu^2)}{2r} \quad (1)$$

where ν is the assumed Poisson's ratio of a biofilm ($\nu = 0.5$)²⁷ and r is the radius of the geometry. The slope is of the force–displacement curve, and was taken at the lower linear region corresponding to 0–30% strain where $R^2 \geq 0.9$.

Spinning-disc rheology. To normalize for differences in biofilm thickness across replicates, prior to analysis, colony-biofilms were compressed to a normal force of 0.01 N. For all analyses a total of 4 biofilms were analyzed, 2 per biological replicate.

Strain sweeps were performed by incrementing the oscillatory strain from 0.01 to 100% at a frequency of 1 Hz. The yield strain was taken where the storage (G') and loss (G'') modulus intersected. Frequency sweeps were performed by incrementing the oscillating frequency from 0.1 to 100 rad/s at a constant strain of 0.1%. This strain was determined to be within the linear viscoelastic region of the strain sweeps for both *Ma*Sm and *Ma*^{Rg} colony-biofilms.

Theoretical mucociliary clearance index (MCI) and cough clearance index (CCI), developed from in vitro models of mucus clearance^{32,33}, were calculated according to Eqs. (2) and (3), respectively, using the relationship between the complex modulus (G^*) and $\tan\delta$ values determined from frequency sweep measurements^{21,22,53}. The MCI and CCI was calculated from values determined at an angular frequency of 1 rad/s and 100 rad/s, respectively.

$$MCI = 1.62 - (0.22 \times \log G_1^*) - (0.77 \times \tan \delta_1) \quad (2)$$

$$CCI = 3.44 - (1.07 \times \log G_{100}^*) + (0.89 \times \tan \delta_{100}) \quad (3)$$

Statistical analysis. Data are presented as mean \pm SD. Statistical significance was determined using either an One-way ANOVA with a Tukey's post-hoc test or a Student's t-test. Analyses were performed using GraphPad Prism v.7 (Graphpad Software). Statistical significance was determined using a p-value < 0.05 .

Data availability

All data generated or analysed during this study are included in this published article (and its Supplementary Information files).

Received: 21 October 2020; Accepted: 10 February 2021

Published online: 03 March 2021

References

- Lam, J., Chan, R., Lam, K. & Costerton, J. W. Production of mucoid microcolonies by *Pseudomonas aeruginosa* within infected lungs in cystic fibrosis. *Infect. Immun.* **28**, 546–556 (1980).
- Singh, P. K. *et al.* Quorum-sensing signals indicate that cystic fibrosis lungs are infected with bacterial biofilms. *Nature* **407**, 762–764. <https://doi.org/10.1038/35037627> (2000).
- Park, I. K. & Olivier, K. N. *Seminars in Respiratory and Critical Care Medicine* 217 (NIH Public Access).
- Furukawa, B. S. & Flume, P. A. *Seminars in Respiratory and Critical Care Medicine* 383–391 (Thieme Medical Publishers, New York, 2018).
- Foundation, C. F. *Cystic Fibrosis Foundation Patient Registry; 2018 Annual Data Report*. (Bethesda, Maryland, 2019).
- Swenson, C., Zerbe, C. S. & Fennelly, K. Host variability in NTM disease: implications for research needs. *Front. Microbiol.* **9**, 2901 (2018).
- Floto, R. A. *et al.* Audit, research and guideline update: US Cystic Fibrosis Foundation and European Cystic Fibrosis Society consensus recommendations for the management of non-tuberculous mycobacteria in individuals with cystic fibrosis: executive summary. *Thorax* **71**, 88 (2016).
- Daniel-Wayman, S. *et al.* Advancing translational science for pulmonary nontuberculous mycobacterial infections. A road map for research. *Am. J. Respir. Crit. Care Med.* **199**, 947–951 (2019).
- Scott, J. P., Ji, Y., Kannan, M. & Wylam, M. E. Inhaled granulocyte–macrophage colony-stimulating factor for *Mycobacterium abscessus* in cystic fibrosis. *Eur. Respir. J.* **51**, 1702127 (2018).
- Wu, M.-L., Aziz, D. B., Dartois, V. & Dick, T. NTM drug discovery: status, gaps and the way forward. *Drug Discov. Today* **23**, 1502–1519 (2018).
- Clary, G. *et al.* *Mycobacterium abscessus* smooth and rough morphotypes form antimicrobial-tolerant biofilm phenotypes but are killed by acetic acid. *Antimicrob. Agents Chemother.* **62**, e01782–e11717 (2018).
- Rhoades, E. R. *et al.* *Mycobacterium abscessus* glycopeptidolipids mask underlying cell wall phosphatidyl-myo-inositol mannosides blocking induction of human macrophage TNF- α by preventing interaction with TLR2. *J. Immunol.* **183**, 1997–2007 (2009).
- Kolpen, M. *et al.* Biofilms of *Mycobacterium abscessus* complex can be sensitized to antibiotics by disaggregation and oxygenation. *Antimicrob. Agents Chemother.* **64**, e01212 (2020).
- Yam, Y.-K., Alvarez, N., Go, M.-L. & Dick, T. Extreme drug tolerance of *Mycobacterium abscessus* “Persisters”. *Front. Microbiol.* **11**, 359 (2020).
- Gloag, E. S., Fabbri, S., Wozniak, D. J. & Stoodley, P. Biofilm mechanics: Implications in infection and survival. *Biofilm* <https://doi.org/10.1016/j.biofm.2019.100017> (2019).
- Branda, S. S., Vik, A., Friedman, L. & Kolter, R. Biofilms: the matrix revisited. *Trends Microbiol.* **13**, 20–26 (2005).
- Gloag, E. S., German, G. K., Stoodley, P. & Wozniak, D. J. Viscoelastic properties of *Pseudomonas aeruginosa* variant biofilms. *Sci. Rep.* **8**, 9691. <https://doi.org/10.1038/s41598-018-28009-5> (2018).
- Kovach, K. *et al.* Evolutionary adaptations of biofilms infecting cystic fibrosis lungs promote mechanical toughness by adjusting polysaccharide production. *Npj Biofilms Microbiomes* **3**, 1 (2017).
- Peterson, B. W. *et al.* Viscoelasticity of biofilms and their recalcitrance to mechanical and chemical challenges. *FEMS Microbiol. Rev.* **39**, 234–245 (2015).
- Klapper, L., Rupp, C. J., Cargo, R., Purvedorj, B. & Stoodley, P. Viscoelastic fluid description of bacterial biofilm material properties. *Biotechnol. Bioeng.* **80**, 289–296. <https://doi.org/10.1002/bit.10376> (2002).
- King, M. Relationship between mucus viscoelasticity and ciliary transport in guaran gel/frog palate model system. *Biorheology* **17**, 249 (1980).
- King, M., Brock, G. & Lundell, C. Clearance of mucus by simulated cough. *J. Appl. Physiol.* **58**, 1776–1782 (1985).
- Ciofu, O., Tolker-Nielsen, T., Jensen, P. O., Wang, H. & Hoiby, N. Antimicrobial resistance, respiratory tract infections and role of biofilms in lung infections in cystic fibrosis patients. *Adv. Drug Deliv. Rev.* **85**, 7–23. <https://doi.org/10.1016/j.addr.2014.11.017> (2015).
- Howard, S. T. *et al.* Spontaneous reversion of *Mycobacterium abscessus* from a smooth to a rough morphotype is associated with reduced expression of glycopeptidolipid and reacquisition of an invasive phenotype. *Microbiology (Reading, England)* **152**, 1581–1590 (2006).
- Nessar, R., Reyrat, J.-M., Davidson, L. B. & Byrd, T. F. Deletion of the mmpL4b gene in the *Mycobacterium abscessus* glycopeptidolipid biosynthetic pathway results in loss of surface colonization capability, but enhanced ability to replicate in human macrophages and stimulate their innate immune response. *Microbiology (Reading, England)* **157**, 1187–1195 (2011).
- Devaraj, A. *et al.* The extracellular DNA lattice of bacterial biofilms is structurally related to Holliday junction recombination intermediates. *Proc. Natl. Acad. Sci. USA* **116**, 25068–25077 (2019).
- Rmaile, A. *et al.* Microbial tribology and disruption of dental plaque bacterial biofilms. *Wear* **306**, 276–284 (2013).
- Stoodley, P., Lewandowski, Z., Boyle, J. D. & Lappin-Scott, H. M. Structural deformation of bacterial biofilms caused by short-term fluctuations in fluid shear: an in situ investigation of biofilm rheology. *Biotechnol. Bioeng.* **65**, 83–92 (1999).
- Fabbri, S. *et al.* Streptococcus mutans biofilm transient viscoelastic fluid behaviour during high-velocity microsprays. *J. Mech. Behav. Biomed. Mater.* **59**, 197–206 (2016).
- Chen, Y., Norde, W., van der Mei, H. C. & Busscher, H. J. Bacterial cell surface deformation under external loading. *mBio* **3**, e00378–e1312 (2012).

31. Ferry, J. D. *Viscoelastic Properties of Polymers* (Wiley, New York, 1980).
32. Grumbein, S., Opitz, M. & Lielig, O. Selected metal ions protect *Bacillus subtilis* biofilms from erosion. *Metallomics* **6**, 1441–1450 (2014).
33. Lielig, O., Caldara, M., Baumgärtel, R. & Ribbeck, K. Mechanical robustness of *Pseudomonas aeruginosa* biofilms. *Soft Matter* **7**, 3307–3314 (2011).
34. Pavlovsky, L., Younger, J. G. & Solomon, M. J. *In situ* rheology of *Staphylococcus epidermidis* bacterial biofilms. *Soft Matter* **9**, 122–131. <https://doi.org/10.1039/c2sm27005f> (2013).
35. Wloka, M., Rehage, H., Flemming, H.-C. & Wingender, J. Structure and rheological behaviour of the extracellular polymeric substance network of mucoid *Pseudomonas aeruginosa* biofilms. *Biofilms* **2**, 275–283 (2005).
36. Yan, J. *et al.* Bacterial biofilm material properties enable removal and transfer by capillary peeling. *Adv. Mater.* **30**, 1804153 (2018).
37. Waters, M. S., Kundu, S., Lin, N. J. & Lin-Gibson, S. Microstructure and mechanical properties of in situ *Streptococcus mutans* biofilms. *ACS Appl. Mater. Interfaces*. **6**, 327–332. <https://doi.org/10.1021/am404344h> (2014).
38. Cense, A. W. *et al.* Mechanical properties and failure of *Streptococcus mutans* biofilms, studied using a microindentation device. *J. Microbiol. Methods* **67**, 463–472. <https://doi.org/10.1016/j.mimet.2006.04.023> (2006).
39. Houari, A. *et al.* Rheology of biofilms formed at the surface of NF membranes in a drinking water production unit. *Biofouling* **24**, 235–240. <https://doi.org/10.1080/08927010802023764> (2008).
40. Di Stefano, A. *et al.* Viscoelastic properties of *Staphylococcus aureus* and *Staphylococcus epidermidis* mono-microbial biofilms. *Microb. Biotechnol.* **2**, 634–641 (2009).
41. Rupp, C. J., Fux, C. A. & Stoodley, P. Viscoelasticity of *Staphylococcus aureus* biofilms in response to fluid shear allows resistance to detachment and facilitates rolling migration. *Appl. Environ. Microbiol.* **71**, 2175–2178 (2005).
42. Marriott, C. Mucus and mucociliary clearance in the respiratory tract. *Adv. Drug Deliv. Rev.* **5**, 19–35. [https://doi.org/10.1016/0169-409X\(90\)90005-D](https://doi.org/10.1016/0169-409X(90)90005-D) (1990).
43. King, M. Interrelation between mechanical properties of mucus and mucociliary transport: Effect of pharmacologic interventions. *Biorheology* **16**, 57 (1979).
44. Voynow, J. A. & Rubin, B. K. Mucins, mucus, and sputum. *Chest* **135**, 505–512. <https://doi.org/10.1378/chest.08-0412> (2009).
45. King, M. The role of mucus viscoelasticity in cough clearance. *Biorheology* **24**, 589–597 (1986).
46. Ma, J. T., Tang, C., Kang, L., Voynow, J. A. & Rubin, B. K. Cystic fibrosis sputum rheology correlates with both acute and longitudinal changes in lung function. *Chest* **154**, 370–377 (2018).
47. Cipolla, D., Shekunov, B., Blanchard, J. & Hickey, A. Lipid-based carriers for pulmonary products: Preclinical development and case studies in humans. *Adv. Drug Deliv. Rev.* **75**, 53–80 (2014).
48. Messiaen, A.-S., Forier, K., Nelis, H., Braeckmans, K. & Coenye, T. Transport of nanoparticles and tobramycin-loaded liposomes in *Burkholderia cepacia* complex biofilms. *PLoS ONE* **8**, e79220 (2013).
49. Dong, D. *et al.* Distribution and inhibition of liposomes on *Staphylococcus aureus* and *Pseudomonas aeruginosa* biofilm. *PLoS ONE* **10**, e0131806 (2015).
50. Jones, W. L., Sutton, M. P., McKittrick, L. & Stewart, P. S. Chemical and antimicrobial treatments change the viscoelastic properties of bacterial biofilms. *Biofouling* **27**, 207–215. <https://doi.org/10.1080/08927014.2011.554977> (2011).
51. Schindelin, J. *et al.* Fiji: An open-source platform for biological-image analysis. *Nat. Methods* **9**, 676 (2012).
52. Timoshenko, S. & Goodier, J. *Theory of Elasticity* 3rd edn. (McGraw Hill Higher Education, New York, 1970).
53. Zayas, J. G., Man, G. C. & King, M. Tracheal mucus rheology in patients undergoing diagnostic bronchoscopy. *Am. Rev. Respir. Dis.* **141**, 1107–1113 (1990).
54. Dasgupta, B. & King, M. Reduction in viscoelasticity in cystic fibrosis sputum in vitro using combined treatment with nacystelyn and rhDNase. *Pediatr. Pulmonol.* **22**, 161–166. [https://doi.org/10.1002/\(sici\)1099-0496\(199609\)22:3](https://doi.org/10.1002/(sici)1099-0496(199609)22:3) (1996).

Acknowledgements

Funding to LHS was provided by the Ohio State University College of Medicine Office of Research Bridge Funding Program and by the Cystic Fibrosis Foundation (HALLST1810). ESG was funded by an American Heart Association Career Development Award (19CDA34630005). DJW and PS were funded by the National Institute of Health (R01AI134895 and R01AI143916; DJW) (R01GM124436; PS).

Author contributions

E.S.G. and L.H.S. developed the hypothesis, designed the study, and performed the experiments. E.S.G., L.H.S. and P.S. performed the data analysis and interpretation. E.S.G., L.H.S., D.J.W. and P.S. wrote the manuscript.

Competing interests

The authors declare no competing interests.

Additional information

Supplementary Information The online version contains supplementary material available at <https://doi.org/10.1038/s41598-021-84525-x>.

Correspondence and requests for materials should be addressed to L.H.-S.

Reprints and permissions information is available at www.nature.com/reprints.

Publisher's note Springer Nature remains neutral with regard to jurisdictional claims in published maps and institutional affiliations.



Open Access This article is licensed under a Creative Commons Attribution 4.0 International License, which permits use, sharing, adaptation, distribution and reproduction in any medium or format, as long as you give appropriate credit to the original author(s) and the source, provide a link to the Creative Commons licence, and indicate if changes were made. The images or other third party material in this article are included in the article's Creative Commons licence, unless indicated otherwise in a credit line to the material. If material is not included in the article's Creative Commons licence and your intended use is not permitted by statutory regulation or exceeds the permitted use, you will need to obtain permission directly from the copyright holder. To view a copy of this licence, visit <http://creativecommons.org/licenses/by/4.0/>.

© The Author(s) 2021